MODELING OF NONLINEAR LOSSES IN AN INTEGRATED CONTACTLESS POWER SUPPLY FOR MAGNETICALLY LEVITATED ELEVATOR SYSTEMS USING DISCRETE CIRCUIT ELEMENTS

A. K. Putri, R. Appunn and K. Hameyer

Institute of Electrical Machines, RWTH Aachen University, Germany
Email: aryanti.putri@iem.rwth-aachen.de

***Abstract* – A contactless energy transmission system is essential to supply onboard systems of electromagnetically levitated vehicles without physical contact to the guide rail. One of the possibilities to realize a contactless power supply (CPS) is by integrating the primary actuator into the guide rail of an electromagnetic guiding system (MGS). The secondary is mounted on the elevator car. This paper introduces an approach for modeling load dependent nonlinear losses occurring in the guide rail using discrete circuit elements.**

I. INTRODUCTION

Electromagnetically levitated vehicles require a contactless power transmission to supply the onboard components in the moving part with electrical energy without sliding contacts or travelling cables. In a fast moving vehicle, e.g. maglev train, the power transmission is integrated within the drive, advantaging the harmonics produced from the propulsion device mounted to the guide rail [1]. On the contrary in a slow moving elevator system, a separate transmission system is required, since the aforementioned method is not feasible in low frequency operation. This yields further cost and space.

Previous studies to minimize cost and space are based on an integrated solution of guiding and power transmission, where the same flux path is used for both operations [2]. An alternative topology, where two different materials are used for the guiding and power transmission system, is proposed in [3]. The primary side consists of a soft magnetic actuator with coils around its lateral arms, which is integrated into the iron guide rail of a MGS. An identical secondary actuator is mounted on the elevator car. When the position of primary and secondary actuators match, a power transmission is established and e.g. the battery supplying the onboard component on the elevator car can be charged. The described topology at aligned position and the flux density at no-load condition is illustrated in figure 1.

By using a suitable reactive power compensation topology, an efficiency of over 90 % in the designed operating point of the CPS may be reached. However, due to leakage flux paths penetrating the guide rail, load dependent additional losses occur in the system. These nonlinear losses can not be modeled utilizing the classic model of iron losses, which is usually an equivalent parallel resistance to the coupling inductance. The other possibility to determine losses in the CPS is using specific iron losses at working frequency and flux density. However, the flux density in the guide rail of operating CPS can not be measured and the losses modeled would be inaccurate. This paper presents a modeling approach of the nonlinear losses using equivalent discrete circuit elements determined by measurements of uncompensated and compensated CPS.

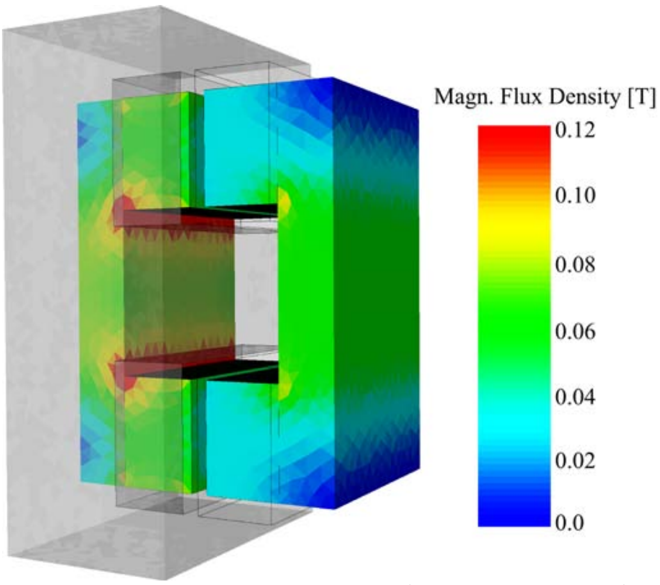

Fig.1. The primary and secondary actuators of the CPS with magnetic flux density at no-load operation.

II. NONLINEAR LOAD DEPENDENT LOSSES

The CPS topology proposed in [3] is constructed and measured. Through no-load measurements the inductance matrix L

$$L = \begin{bmatrix} L_p & M \\ M & L_s \end{bmatrix} \tag{1}$$

is determined. The values of the CPS equivalent circuit elements are listed in table I. Simulated and measured values show a good accordance with maximum deviation of 14.9 % on primary inductance L_p, which means an increase in the primary side leakage flux $\Phi_{\sigma,1}$. The phase shift between voltage and current at no load is 86°. Both indicates additional losses caused by the buried topology of the primary actuator. However, the losses are sufficiently small and can be neglected.

TABLE I
MEASURED AND SIMULATED EQUIVALENT CIRCUIT COMPONENTS

	Simulated	Measured	Deviation
Primary self inductance L_p	47.75 µH	56.11 µH	14.9 %
Secondary self inductance L_s	47.73 µH	52.18 µH	8.5 %
Mutual inductance M	39.53 µH	38.7 µH	2.1 %
Load Resistance	5 Ω	5. 08 Ω	1.6 %

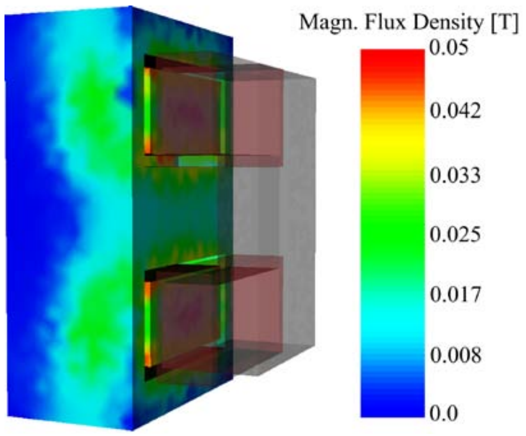

Fig.2. Magnetic flux density within the guide rail in case of opposite currents applied to primary and secondary windings.

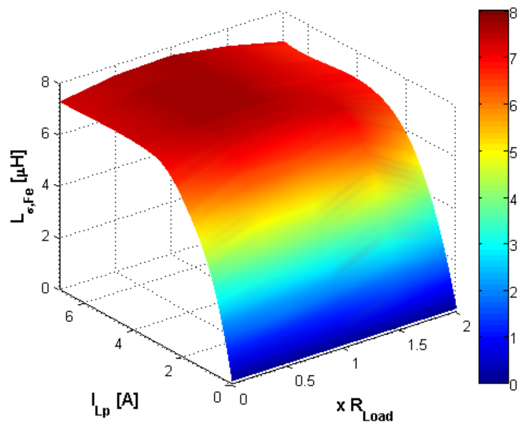

Fig.3. Additional leakage inductance $L_{\sigma Fe}$ of the guide rail.

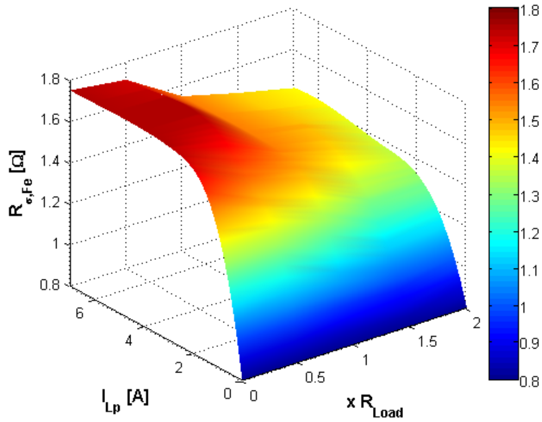

Fig.4. Additional iron resistance $R_{\sigma Fe}$ of the guide rail.

From short circuit measurements a phase shift of 77° is observed. In this operation point the additional losses occur in the iron guide rail can not be neglected. To analyze this phenomenon a FEM simulation is performed with primary and secondary windings powered by 10 A in opposite direction. From figure 2 it can be seen that the flux no longer penetrates only the soft-ferrite actuator, but also the iron guide rail between the yokes of the primary actuator. The mean value of the flux density in the primary actuator and the iron between the yokes is respectively 0.021 T and 0.017 T. The CPS has a high percentage of primary side leakage flux $\Phi_{\sigma,1}$.

III. MODELING APPROACHES

FEM simulations to determine the flux density in the guide rail for various winding current combinations are performed. From the results, it can be concluded, that the primary side leakage flux is a function of primary and secondary current. In an operating CPS the ratio of primary and secondary current is determined by its reflected impedance. If the inductance matrix of the CPS is unchanged, the dependency is limited to the load impedance, or in this case to the battery inner resistance [4]. Considering the behavior of the additional losses, aside the inductance matrix the circuit model of the CPS should consist of at least two additional elements: leakage inductance $L_{\sigma Fe}$, to model the increasing leakage flux, and iron resistance $R_{\sigma Fe}$, to model the losses in the system. Both elements are connected in series and a function of primary current I_p and load resistance R_{load}.

The next step is to determine a feasible model for the CPS. There are three possibilities to arrange the additional circuit elements in an equivalent circuit model of the CPS: on the primary side, on the secondary side, and on both sides, with two elements on each side. Using the analytical equations of the equivalents circuits and the measurement results of an uncompensated CPS with different load resistances and primary winding currents, the accurate model could be chosen. In the analytical equations, a circuit element without certain behavior is used to represent both additional elements.

IV. RESULTS

From the three possibilities of the adjusted equivalent circuit model of the CPS, the model with the additional circuit elements arranged on the primary side shows the most feasible results. In the model with the additional elements on the secondary side and both sides of the CPS, $L_{\sigma Fe}$ and $R_{\sigma Fe}$ become negative at higher and lower load resistance, respectively. Figure 3 and 4 show $L_{\sigma Fe}$ and $R_{\sigma Fe}$ as a function of current through primary inductance I_p and fraction of load resistance R_{load} for the chosen equivalent circuit model. Both additional elements $L_{\sigma Fe}$ and $R_{\sigma Fe}$ increase proportional to I_p until their saturation points at $I_p = 2$ A. The leakage inductance $L_{\sigma Fe}$ has non remarkable load dependency and the iron resistance $R_{\sigma Fe}$ is inversely proportional to the load resistance R_{load}.

V. CONCLUSIONS

In this paper an extended equivalent circuit model of a CPS to model additional iron losses in the guide rail has been introduced. The additional components are current and load dependent leakage inductance $L_{\sigma Fe}$ and iron resistance $R_{\sigma Fe}$. The modelling accuracy of the CPS is thereby increased.

REFERENCES

[1] J.-Y. Lee, I.-J. Lee, J.-W. Kim, J.-H. Chang, D.-H. Kang, S.-U. Chung and J.-P. Hong, "Contactless power transfer system combined with linear electric machine", *Proc. of 8th Int. Conf. on Electrical Machines and Systems (ICEMS 2007)*, Seoul, pp. 1544 –1548, 2007.

[2] R. Appunn, B. Riemer, and K. Hameyer, "Contactless power supply for magnetically levitated elevator systems", *Proc. of 20th Int. Conf. on Electrical Machines (ICEM 2012)*, Marseille, pp. 600 – 605, Sept. 2012.

[3] R. Appunn, A. K. Putri, and K. Hameyer, "Design of a contactless power supply for magnetically levitated elevator systems integrated into the guide rail", *Applied Mechanics and Materials*, vol. 416 – 417, pp. 333 – 338, 2013.

[4] C.-S. Wang, O. H, Stielau and G. A. Covic, "Load models and their application in the design of loosely coupled inductive power transfer systems", *Proc. of Int. Conf.on Power System Technology*, Dez. 2000.